

## Interactions of Tetrakis(4-*N*-methylpyridyl)porphyrin with Cyclodextrins and Disodium Phthalate in Aqueous Solution

SANYO HAMAI\*

*Department of Chemistry, Faculty of Education and Human Studies, Akita University, Tegata Gakuen-machi 1-1, Akita, 010-8502, Japan*

(Received: 5 July 2006; in final form: 15 September 2006)

**Key words:** absorption spectra, fluorescence spectra, cyclodextrins, disodium phthalate, tetrakis(4-*N*-methylpyridyl)porphyrin

### Abstract

In pH 7.3 buffers, the interactions of a cationic porphyrin, tetrakis(4-*N*-methylpyridyl)porphyrin (TMPyP), with cyclodextrins (CDs) and disodium phthalate (DSP) have been examined by means of absorption, fluorescence, and induced circular dichroism spectroscopy.  $\alpha$ -CD,  $\beta$ -CD, and  $\gamma$ -CD form a 1:1 inclusion complex with a TMPyP monomer, which dimerizes in solution without CD. TMPyP also forms a 1:1 organic cation–organic anion complex with DSP. The 1:1 TMPyP–DSP complex forms a ternary CD–TMPyP–DSP inclusion complex with  $\alpha$ -,  $\beta$ -, and  $\gamma$ -CD, in which a DSP molecule is not incorporated into the CD cavity. From the fluorescence intensity change, the equilibrium constants have been evaluated for the formation of the inclusion complexes and the organic cation–anion complexes.

### Introduction

Anionic porphyrins such as tetrakis(4-sulfonatophenyl)porphyrin are readily incorporated into the cyclodextrin (CD) cavity to form inclusion complexes [1–9]. In the porphyrins, the binding sites towards the CD cavity are a benzene-ring moiety substituted on a meso position of a porphyrin ring. On the other hand, cationic porphyrins are known to form little or no inclusion complexes with CDs, although cationic porphyrins, tetrakis(4-*N*-methylpyridyl)porphyrin (TMPyP) and tetrakis(4-*N*-ethylpyridyl)porphyrin, have been reported to form inclusion complexes with CDs [10–12]. A tetraamino porphyrin derivative also forms an inclusion complex with heptakis(2,6-dimethyl)- $\beta$ -CD [13].

When a dimer of a guest molecule interacts with a CD molecule, a guest monomer, which is generated by the dissociation of the guest dimer, tends to be incorporated into the CD cavity. In some cases, however, a guest dimer is incorporated into the CD cavity to form a 1:2 CD–guest inclusion complex [14–16]. In contrast to the dissociation of the dimer, it has been reported that guest monomers dimerize within the CD cavity [14–16]. TMPyP readily dimerizes in dilute TMPyP solution without CD [17].

Organic cations often form complexes with organic anions. There are organic cation–organic anion complexes of 2,6-bis(1-pyridiniummethyl)naphthalene dibromide-2,6-naphthalenedicarboxylate, Methylene Blue–2-naphthalenesulfonate, Methylene Blue–tetrakis(4-sulfonatophenyl)porphyrin, 1,1'-diheptyl-4,4'-bipyridinium dibromide–tetrakis(4-carboxyphenyl)porphyrin, and so on [15, 16, 18–24]. In addition, several organic cation–organic anion complexes form ternary inclusion complexes with CD, although the Methylene Blue–tetrakis(4-sulfonatophenyl)porphyrin complex dissociates into individual components upon the addition of CD [15, 16, 18, 20, 22–24]. In the case of the Methylene Blue–tetrakis(4-sulfonatophenyl)porphyrin complex, a bulky molecule, Methylene Blue, cannot be simultaneously bound to the CD cavity, together with tetrakis(4-sulfonatophenyl)porphyrin [22]. We have found that TMPyP forms an organic cation–organic anion complex with a relatively bulky molecule, disodium phthalate (DSP), which is not as bulky as Methylene Blue.

For cationic porphyrins involving TMPyP, quantitative studies concerning the inclusion of CD have hardly been made. As previously stated, the dimerization of TMPyP at dilute concentrations is distinctive compared to other porphyrins. In CD solution, therefore, TMPyP may behave in a fashion different from the other porphyrins. In addition, the formation of the

\* Author for Correspondence. e-mail: hamai@ipc.akita-u.ac.jp

TMPyP–DSP complex has been found. Under the circumstances, it is worth examining whether the interactions of CD with the TMPyP dimer induce the dissociation of the dimer or not, and whether a ternary inclusion complex is formed or not among  $\gamma$ -CD, TMPyP, and DSP.

Thus, we have investigated the complexation of TMPyP with DSP. In addition, the interactions between CD and TMPyP and those between the CD-TMPyP inclusion complex and DSP have been examined by means of absorption, fluorescence, and circular dichroism spectroscopy.

## Experimental

Tetrakis(4-*N*-methylpyridyl)porphyrin (TMPyP) and disodium phthalate (DSP) were purchased from Tokyo Kasei Kogyo Co. Ltd., and were used as received.

$\alpha$ -Cyclodextrin ( $\alpha$ -CD) and  $\beta$ -CD were obtained from Nacalai Tesque Inc.  $\beta$ -CD was twice recrystallized from water, whereas  $\alpha$ -CD was used as received.  $\gamma$ -CD, which was obtained from Wako Pure Chemical Industries, Ltd., was used without further purification.

Buffers ( $6.7 \times 10^{-4}$  mol dm<sup>-3</sup> of KH<sub>2</sub>PO<sub>4</sub> and  $2.7 \times 10^{-3}$  mol dm<sup>-3</sup> of Na<sub>2</sub>HPO<sub>4</sub>) of pH 7.3 were used throughout this work.

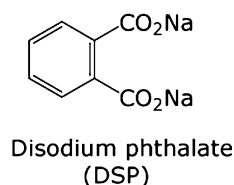
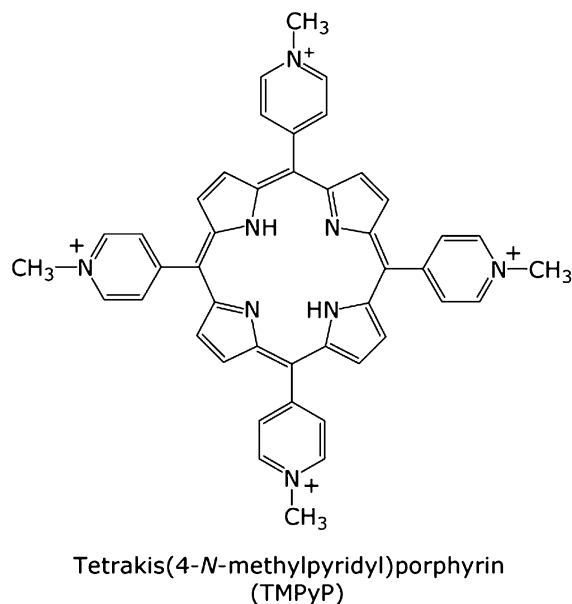


Chart 1. Structural formulas of TMPyP and DSP.

Absorption spectra were recorded on a Shimadzu UV-260 spectrophotometer. Fluorescence spectra were taken with a Shimadzu RF-501 spectrofluorometer equipped with a cooled Hamamatsu R-943 photomultiplier. The fluorescence spectra were corrected for the spectral response of the fluorometer. Induced circular dichroism (icd) spectra were recorded on a JASCO J-400X spectropolarimeter interfaced to a JASCO DP-500 data processor. To obtain the icd spectra, the icd spectral data were accumulated eight times. A reference spectrum of CD solution without TMPyP was similarly measured, and was subtracted from the sample spectra. Spectroscopic measurements were made at  $25 \pm 0.1$  °C, except for the measurements of icd spectra which were recorded at  $25 \pm 2$  °C.

## Results and discussion

### Inclusion interactions of $\gamma$ -CD with TMPyP

Upon the addition of  $\gamma$ -CD, the absorption maximum of TMPyP ( $2.0 \times 10^{-6}$  mol dm<sup>-3</sup>) in pH 7.3 buffers was slightly shifted to longer wavelengths, accompanied by isosbestic points at 421 and 438 nm. The absorption spectral changes indicate the formation of an inclusion complex of  $\gamma$ -CD with TMPyP.

Figure 1 depicts fluorescence spectra of TMPyP ( $2.0 \times 10^{-6}$  mol dm<sup>-3</sup>) in pH 7.3 buffers containing various  $\gamma$ -CD concentrations. When  $\gamma$ -CD is added to TMPyP solution, the TMPyP fluorescence is enhanced in intensity, with a significant sharpening of the fluorescence bands. The fluorescence spectral changes as well as the absorption spectral changes indicate the formation of the inclusion complex between  $\gamma$ -CD and TMPyP.

Figure 2 illustrates fluorescence spectra for a dilute TMPyP solution ( $2.0 \times 10^{-8}$  mol dm<sup>-3</sup>) in the absence

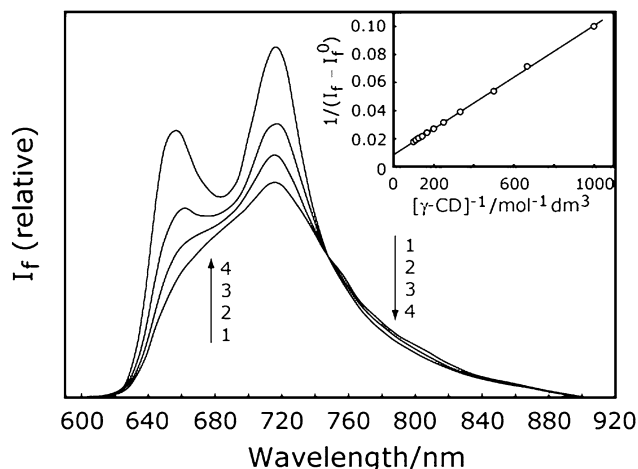


Figure 1. Fluorescence spectra of TMPyP ( $2.0 \times 10^{-6}$  mol dm<sup>-3</sup>) in pH 7.3 buffers containing various concentrations of  $\gamma$ -CD. Concentration of  $\gamma$ -CD: (1) 0, (2)  $1.0 \times 10^{-3}$ , (3)  $3.0 \times 10^{-3}$ , and (4)  $1.0 \times 10^{-2}$  mol dm<sup>-3</sup>.  $\lambda_{\text{ex}} = 421$  nm. The inset shows the double reciprocal plot for the fluorescence intensity of TMPyP ( $2.0 \times 10^{-6}$  mol dm<sup>-3</sup>) in pH 7.3 buffers containing  $\gamma$ -CD.  $\lambda_{\text{ex}} = 421$  nm.  $\lambda_{\text{obs}} = 660$  nm.

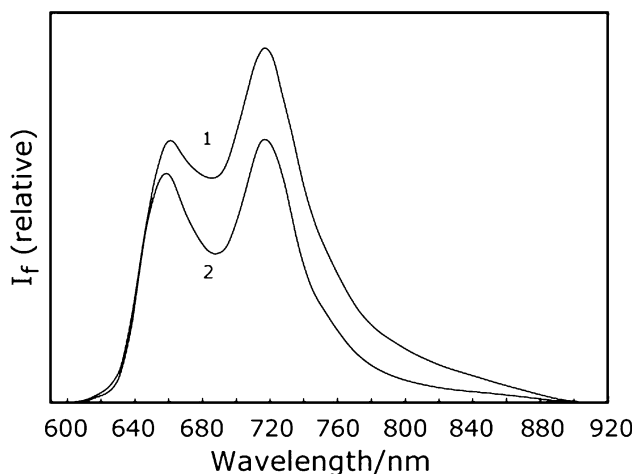


Figure 2. Fluorescence spectra of TMPyP ( $2.0 \times 10^{-8} \text{ mol dm}^{-3}$ ) in pH 7.3 buffers in the absence (spectrum 1) and presence (spectrum 2) of  $\gamma$ -CD ( $1.0 \times 10^{-2} \text{ mol dm}^{-3}$ ).  $\lambda_{\text{ex}} = 421 \text{ nm}$ .

and presence of  $\gamma$ -CD ( $1.0 \times 10^{-2} \text{ mol dm}^{-3}$ ). In the absence of  $\gamma$ -CD, the fluorescence spectrum at a higher concentration ( $2.0 \times 10^{-6} \text{ mol dm}^{-3}$ ) (Figure 1) shows a broad band with a shoulder at about 660 nm, while the fluorescence spectrum at a low concentration ( $2.0 \times 10^{-8} \text{ mol dm}^{-3}$ ) (Figure 2) shows two sharp peaks. The difference in the fluorescence spectra indicates that TMPyP dimerizes even at low concentrations such as  $2.0 \times 10^{-6} \text{ mol dm}^{-3}$ . The dimerization of TMPyP at  $2.0 \times 10^{-6} \text{ mol dm}^{-3}$  is in agreement with the result obtained by Kano et al. [17].



Here,  $K_2$  is the equilibrium constant for the formation of the TMPyP dimer ( $(\text{TMPyP})_2$ ). At a low concentration of TMPyP, its fluorescence intensity in the presence of  $\gamma$ -CD is reduced with a sharpening of the fluorescence bands. The reduction in the fluorescence intensity upon the addition of  $\gamma$ -CD is in contrast to the enhancement of the fluorescence intensity at  $2.0 \times 10^{-6} \text{ mol dm}^{-3}$  of TMPyP upon the addition of  $\gamma$ -CD. Figure 3 exhibits the dependence of the fluorescence intensity observed at 660 nm on the TMPyP concentration. The fluorescence intensity of TMPyP,  $I_f$ , is represented by

$$I_f = (a + bK_2 [\text{TMPyP}]) [\text{TMPyP}] \quad (2)$$

where  $a$  and  $b$  are the experimental constants including the fluorescence quantum yields of the TMPyP monomer and dimer, respectively. Figure 3 also shows the best fit simulation curve, for which  $a$ ,  $b$ , and  $K_2$  are assumed to be  $3.48 \times 10^9$ ,  $3.60 \times 10^{12}$ , and  $4060 \text{ mol}^{-1} \text{ dm}^3$ , respectively. The  $K_2$  value for TMPyP is considerably less than that ( $1.70 \times 10^5 \text{ mol}^{-1} \text{ dm}^3$ ) for hematoporphyrin [24]. The finding that the  $a$  value is three orders of magnitude less than the  $b$  value indicates that the TMPyP monomer fluorescence is significantly weaker in intensity than the TMPyP dimer fluorescence. This is the reason why the dimer is detected in spite of the relatively small  $K_2$  value.

As previously stated, the fluorescence intensity at a low TMPyP concentration is reduced by the addition of  $\gamma$ -CD. The addition of  $\gamma$ -CD decreases the TMPyP dimer concentration, because of the formation of the  $\gamma$ -CD-TMPyP inclusion complex. The concentration ratio,  $[(\text{TMPyP})_2]/[\text{TMPyP}]$ , at a low TMPyP concentration is smaller than that at a high TMPyP concentration. At low TMPyP concentrations, therefore,  $\gamma$ -CD causes the more prominent decrease in the concentration ratio, compared to at high TMPyP concentrations. Because the fluorescence intensity of the TMPyP dimer is significantly stronger than that of the TMPyP monomer, the addition of  $\gamma$ -CD leads to the reduction in the fluorescence intensity at a low TMPyP concentration, although the fluorescence intensity of the  $\gamma$ -CD-TMPyP inclusion complex is stronger than that of free TMPyP (v. i.).

The inset of Figure 1 shows the double reciprocal plot for the fluorescence intensity of TMPyP ( $2.0 \times 10^{-6} \text{ mol dm}^{-3}$ ) in  $\gamma$ -CD solution. From the plot, an equilibrium constant ( $K_1$ ) for the formation of the inclusion complex of  $\gamma$ -CD with TMPyP is estimated to be  $94 \pm 3 \text{ mol}^{-1} \text{ dm}^3$ . This  $K_1$  value for TMPyP is significantly less than the  $K_1$  values ( $1600 \pm 200$  and  $5600 \pm 300 \text{ mol}^{-1} \text{ dm}^3$ ) of  $\gamma$ -CD for tetrakis(4-sulfonatophenyl)porphyrin and tetrakis(4-carboxyphenyl)porphyrin, respectively, which represent the equilibrium constant for the formation of the 1:1  $\gamma$ -CD-porphyrin monomer inclusion complex [4, 23]. The significantly small  $K_1$  value for TMPyP is consistent with the result reported by Kano et al [10]. The straight line in the inset of Figure 1 well fits the observed data, indicating that the inclusion complex is a 1:1  $\gamma$ -CD-TMPyP monomer inclusion complex or a 1:1  $\gamma$ -CD-TMPyP dimer inclusion complex. When the 1:1  $\gamma$ -CD-TMPyP monomer inclusion complex is formed, a TMPyP dimer dissociates to the monomers, followed by the incorporation of the monomer into the  $\gamma$ -CD cavity to form the inclusion complex.

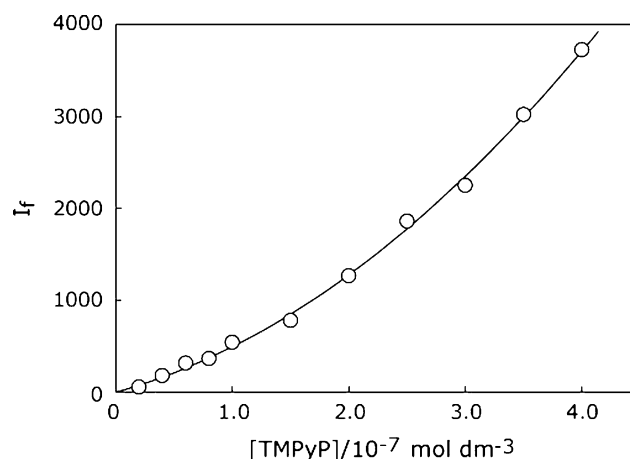
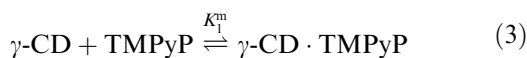


Figure 3. Simulation for the observed fluorescence intensities of TMPyP as a function of the TMPyP concentration.  $\lambda_{\text{ex}} = 421 \text{ nm}$ .  $\lambda_{\text{obs}} = 660 \text{ nm}$ .



where  $K_1^m$  are the equilibrium constant for the formation of the 1:1  $\gamma\text{-CD}$ -TMPyP monomer inclusion complex ( $\gamma\text{-CD} \cdot \text{TMPyP}$ ).

In this scheme, the fluorescence intensity under our experimental conditions is expressed as

$$I_f = c[\text{TMPyP}] + d[\gamma\text{-CD} \cdot \text{TMPyP}] + e[(\text{TMPyP})_2] \quad (4)$$

$$= (c + dK_1^m[\gamma\text{-CD}] + eK_2[\text{TMPyP}])[\text{TMPyP}]$$

where  $c$ ,  $d$ , and  $e$  are the constants including the fluorescence quantum yields of the TMPyP monomer, the 1:1  $\gamma\text{-CD}$ -TMPyP monomer inclusion complex, and the TMPyP dimer, respectively. The value of  $e/c$  is equal to the value of  $b/a$  (1034) at the same excitation wavelength of 421 nm. Consequently, Equation (4) is rewritten as

$$I_f = (c + dK_1^m[\gamma\text{-CD}] + 1034cK_2[\text{TMPyP}])[\text{TMPyP}] \quad (5)$$

The initial concentration of TMPyP,  $[\text{TMPyP}]_0$ , is given by

$$[\text{TMPyP}]_0 = [\text{TMPyP}] + [\gamma\text{-CD} \cdot \text{TMPyP}] + 2[(\text{TMPyP})_2]$$

$$= (1 + K_1^m[\gamma\text{-CD}] + 2K_2[\text{TMPyP}])[\text{TMPyP}] \quad (6)$$

Consequently, the following quadratic equation holds for the concentration of the TMPyP monomer.

$$2K_2[\text{TMPyP}]^2 + (1 + K_1^m[\gamma\text{-CD}])[\text{TMPyP}] - [\text{TMPyP}]_0 = 0 \quad (7)$$

The  $K_2$  value has already been evaluated from the TMPyP concentration dependence of the fluorescence intensity. Because the concentration of the TMPyP monomer can be calculated using an assumed value of  $K_1^m$ , the fluorescence intensity is evaluated from Equation (5), using variables,  $c$  and  $d$ . Figure 4 shows the observed fluorescence intensity data as a function of the  $\gamma\text{-CD}$  concentration, together with the best fit simulation curve calculated on the basis of Equation (5), for which the values of  $c$ ,  $d$ , and  $K_1^m$  are assumed to be  $2.40 \times 10^6$ ,  $7.65 \times 10^7$ , and  $148 \text{ mol}^{-1} \text{ dm}^3$ , respectively. This  $K_1^m$  value is close to the  $K_1$  value ( $94 \pm 3 \text{ mol}^{-1} \text{ dm}^3$ ) obtained from the double-reciprocal plot. This finding suggests that  $\gamma\text{-CD}$  forms a 1:1 inclusion complex with the TMPyP monomer. In this study, we have used the  $K_1$  value obtained from the double-reciprocal plot as the equilibrium constant for the formation of the 1:1  $\gamma\text{-CD}$ -TMPyP inclusion complex, because the number of parameters for the double-reciprocal plot is less than that for the simulation method and because the straight line in the double-reciprocal plot well fits the observed data.

To confirm the above scheme that  $\gamma\text{-CD}$  accommodates the TMPyP monomer, we simulated the fluorescence intensity under the assumption that  $\gamma\text{-CD}$  forms an inclusion complex with the TMPyP dimer.

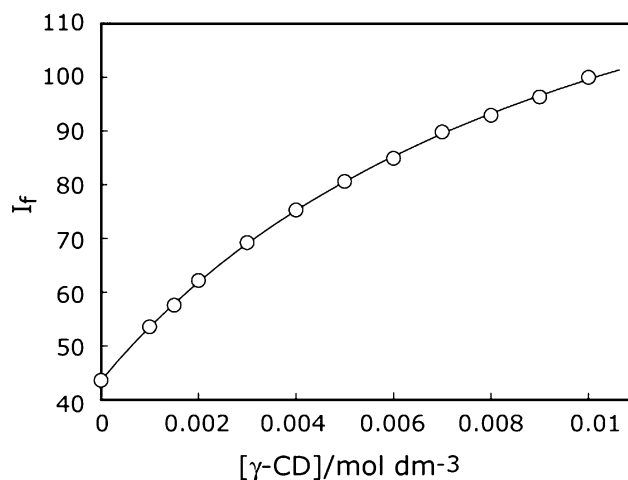
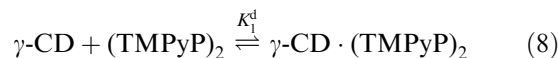


Figure 4. Simulation for the observed fluorescence intensities of TMPyP solution containing  $\gamma\text{-CD}$ .  $\lambda_{\text{ex}} = 421 \text{ nm}$ .  $\lambda_{\text{obs}} = 660 \text{ nm}$ .



Here,  $K_1^d$  is the equilibrium constant for the formation of the 1:1  $\gamma\text{-CD}$ -TMPyP dimer inclusion complex ( $\gamma\text{-CD} \cdot (\text{TMPyP})_2$ ). In this case, the simulation has afforded a  $K_1^d$  value of  $6330 \text{ mol}^{-1} \text{ dm}^3$  (not shown), which is about 70 times greater than the  $K_1$  value obtained from the double-reciprocal plot. This supports that  $\gamma\text{-CD}$  interacts with the TMPyP monomer to form the 1:1  $\gamma\text{-CD}$ -TMPyP monomer inclusion complex.

Absorption and fluorescence spectral changes similar to those for  $\gamma\text{-CD}$  have been observed for  $\alpha$ - and  $\beta$ -CD. Although the cavity sizes of  $\alpha$ - and  $\beta$ -CD are less than that of  $\gamma$ -CD,  $K_1$  values of  $74 \pm 7$  and  $110 \pm 10 \text{ mol}^{-1} \text{ dm}^3$ , which are nearly the same as the  $K_1$  value for  $\gamma$ -CD, have been obtained for  $\alpha$ - and  $\beta$ -CD, respectively. Nearly the same and small  $K_1$  values for  $\alpha$ -,  $\beta$ - and  $\gamma$ -CD may suggest that an *N*-methylpyridyl moiety of TMPyP is relatively shallowly bound to the CD cavity.

#### Complex formation of TMPyP with DSP

When DSP was added to TMPyP ( $2.0 \times 10^{-6} \text{ mol dm}^{-3}$ ) solution (pH 7.3), the absorption maximum was shifted to longer wavelengths, accompanied by an isosbestic point at 426 nm. In contrast to  $\gamma\text{-CD}$ , the absorption maximum was decreased in intensity, as the DSP concentration was increased. The absorption spectral changes by the addition of DSP indicate the formation of an organic cation-organic anion complex between TMPyP and DSP. Figure 5 shows fluorescence spectra of TMPyP ( $2.0 \times 10^{-6} \text{ mol dm}^{-3}$ ) in pH 7.3 buffers containing various concentrations of DSP. Upon the addition of DSP, the fluorescence intensity is enhanced with a sharpening of the fluorescence bands, although the sharpening is not as significant as that (Figure 1) upon the addition of  $\gamma\text{-CD}$ . The fluorescence spectral change also indicates the formation of the complex between TMPyP and



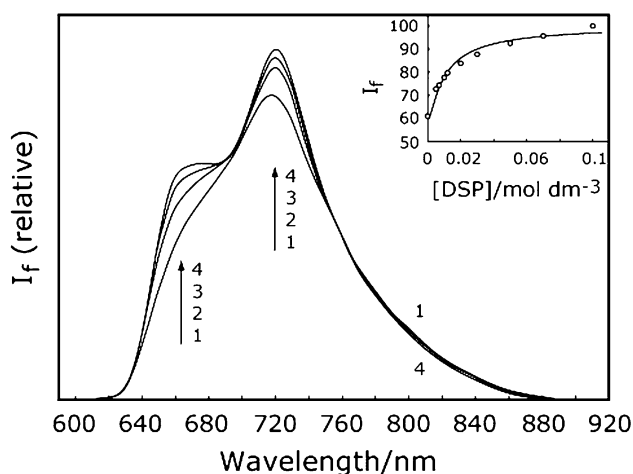


Figure 5. Fluorescence spectra of TMPyP ( $2.0 \times 10^{-6} \text{ mol dm}^{-3}$ ) in pH 7.3 buffers containing various concentrations of DSP. Concentration of DSP: (1) 0, (2)  $1.0 \times 10^{-2}$ , (3)  $3.0 \times 10^{-2}$ , and (4)  $1.0 \times 10^{-1} \text{ mol dm}^{-3}$ .  $\lambda_{\text{ex}} = 426 \text{ nm}$ . The inset shows the simulation for the observed fluorescence intensities of TMPyP solution containing DSP.  $[\text{TMPyP}]_0 = 2.0 \times 10^{-6} \text{ mol dm}^{-3}$ .  $\lambda_{\text{ex}} = 426 \text{ nm}$ .  $\lambda_{\text{obs}} = 660 \text{ nm}$ .

DSP. As the DSP concentration was increased in dilute TMPyP solutions ( $2.0 \times 10^{-8} \text{ mol dm}^{-3}$ ), the TMPyP fluorescence was remarkably enhanced in intensity, accompanied by a sharpening of the fluorescence band (not shown). The fluorescence spectral change at a TMPyP concentration of  $2.0 \times 10^{-8} \text{ mol dm}^{-3}$  has been prominent compared to that in Figure 5 ( $2.0 \times 10^{-6} \text{ mol dm}^{-3}$ ), indicating the existence of the monomer–dimer equilibrium of TMPyP. This conclusion is in agreement with the result obtained from the fluorescence spectral change by the addition of  $\gamma$ -CD. As in the case of the inclusion complex of  $\gamma$ -CD with TMPyP, the TMPyP monomer most likely forms the organic cation–organic anion complex with DSP:



where  $K_3$  is the equilibrium constant for the formation of the 1:1 TMPyP monomer–DSP complex (TMPyP · DSP). The fluorescence intensity is represented as

$$I_f = f[\text{TMPyP}] + g[(\text{TMPyP})_2] + h[\text{TMPyP} \cdot \text{DSP}] \\ = (f + gK_2[\text{TMPyP}] + hK_3[\text{DSP}])([\text{TMPyP}]) \quad (10)$$

Here,  $f$ ,  $g$ , and  $h$  are the constants including the fluorescence quantum yields for the TMPyP monomer, TMPyP dimer, and the TMPyP monomer–DSP complex, respectively. As in the case of the ratio  $b/a$ , the ratio  $g/f$  has been evaluated to be 1080 at an excitation wavelength of 426 nm. Under the assumption of a  $K_3$  value, the concentration of the TMPyP monomer is given by solving the quadratic equation.

$$2K_2[\text{TMPyP}]^2 + (1 + K_3[\text{DSP}])([\text{TMPyP}]) - [\text{TMPyP}]_0 = 0 \quad (11)$$

Consequently, the fluorescence intensity can be calculated employing assumed values of  $f$ ,  $h$ , and  $K_3$ . The best fit simulation curve ( $\text{SD} = 0.5860$ ), for which  $f = 3.25 \times 10^6$ ,  $h = 5.03 \times 10^7$ , and  $K_3 = 242 \text{ mol}^{-1} \text{ dm}^3$  are assumed, is exhibited in the inset of Figure 5, in which the observed fluorescence intensities are also shown. When a simulation was performed on the basis of another scheme, which involved the 1:2 TMPyP–DSP complex as well as the 1:1 TMPyP–DSP complex, the best fit simulation curve ( $\text{SD} = 0.3290$ ) well fitted the observed data (not shown), except for the curve near the zero DSP concentration. Consequently, there may be the possibility that the 1:2 TMPyP–DSP complex also exists in TMPyP solution containing DSP. Under the assumption that the 1:2 TMPyP–DSP complex alone is formed, the best fit simulation curve has not reproduced the observed data ( $\text{SD} = 4.155$ ) (not shown). This result indicates the 1:1 TMPyP–DSP complex is the major species.

#### Complex formation in the $\gamma$ -CD–TMPyP–DSP system

There was little or no absorption spectral change of DSP upon the addition of  $\gamma$ -CD. Consequently, DSP seems to hardly form an inclusion complex with  $\gamma$ -CD. When DSP was added to TMPyP ( $2.0 \times 10^{-6} \text{ mol dm}^{-3}$ ) solution (pH 7.3) containing  $\gamma$ -CD ( $3.0 \times 10^{-3} \text{ mol dm}^{-3}$ ), the absorption band was shifted to longer wavelengths. Below about  $3.0 \times 10^{-2} \text{ mol dm}^{-3}$  of DSP, an isosbestic point was observed at 426 nm, which was the same wavelength as that of the isosbestic point in the TMPyP–DSP system without  $\gamma$ -CD. Above about  $3.0 \times 10^{-2} \text{ mol dm}^{-3}$ , however, an isosbestic point did not appear, suggesting that another species, a ternary inclusion complex formed among  $\gamma$ -CD, TMPyP, and DSP, existed besides the  $\gamma$ -CD–TMPyP inclusion complex and the TMPyP–DSP complex. In the ternary  $\gamma$ -CD–TMPyP–DSP inclusion complex, the TMPyP monomer is most likely involved, because  $\gamma$ -CD interacts with the TMPyP monomer to form a 1:1 inclusion complex.

Figure 6 illustrates fluorescence spectra of TMPyP ( $2.0 \times 10^{-6} \text{ mol dm}^{-3}$ ) in pH 7.3 buffers containing  $\gamma$ -CD ( $3.0 \times 10^{-3} \text{ mol dm}^{-3}$ ) and several concentrations of DSP. In contrast to the fluorescence spectra in Figure 5, in which  $\gamma$ -CD is not involved, the fluorescence maximum at about 660 nm becomes considerably sharp upon the addition of DSP. This fluorescence spectral change supports the existence of the  $\gamma$ -CD–TMPyP–DSP inclusion complex. To further confirm the existence of the  $\gamma$ -CD–TMPyP–DSP inclusion complex, icd spectra of TMPyP were measured in pH 7.3 buffers containing  $\gamma$ -CD and DSP (Figure 7). The negative icd signal is observed for TMPyP in  $\gamma$ -CD solution. The negative signal for TMPyP is in contrast to the positive signals for tetrakis(4-sulfonatophenyl)porphyrin and tetrakis(4-carboxyphenyl)porphyrin in  $\gamma$ -CD solution [4, 23]. At present, the reason why the icd signal sign is

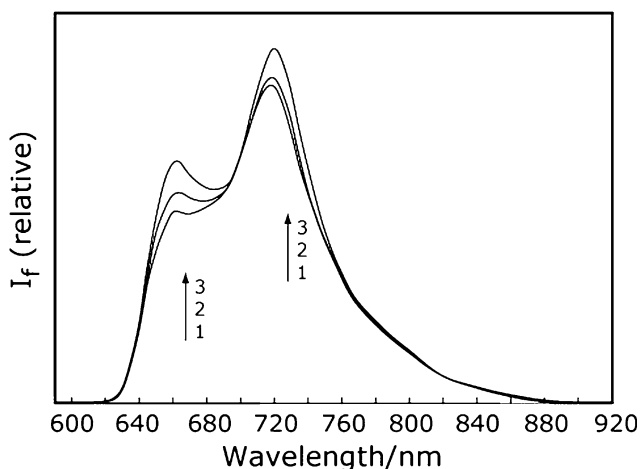
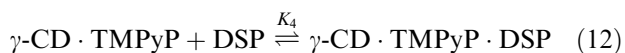


Figure 6. Fluorescence spectra of TMPyP ( $2.0 \times 10^{-6} \text{ mol dm}^{-3}$ ) in pH 7.3 buffers containing  $\gamma$ -CD ( $3.0 \times 10^{-3} \text{ mol dm}^{-3}$ ) and several concentrations of DSP. Concentration of DSP: (1) 0, (2)  $1.0 \times 10^{-2}$ , and (3)  $1.0 \times 10^{-1} \text{ mol dm}^{-3}$ .  $\lambda_{\text{ex}} = 426 \text{ nm}$ .

different between TMPyP and the anionic porphyrins is not clear. In the inclusion by  $\gamma$ -CD, however, the penetration depth and/or orientation of TMPyP within the  $\gamma$ -CD cavity are/is different from those/that of the anionic porphyrins. At  $3.0 \times 10^{-3}$  and  $1.0 \times 10^{-2} \text{ mol dm}^{-3}$  of  $\gamma$ -CD, the icd signal intensity of TMPyP decreases by at most 10% upon the addition of DSP ( $0.1 \text{ mol dm}^{-3}$ ). The  $K_1$  value ( $94 \text{ mol}^{-1} \text{ dm}^3$ ) for the formation of the  $\gamma$ -CD-TMPyP inclusion complex is less than half of the  $K_3$  value ( $242 \text{ mol}^{-1} \text{ dm}^3$ ) for the formation of the TMPyP-DSP complex. The  $\gamma$ -CD concentration used is one to two orders of magnitude less than the concentration of DSP added. If the ternary  $\gamma$ -CD-TMPyP-DSP inclusion complex is not formed in TMPyP solution containing  $\gamma$ -CD and DSP (only the  $\gamma$ -CD-TMPyP and TMPyP-DSP complexes are present), the concentration of the  $\gamma$ -CD-TMPyP inclusion complex at  $\gamma$ -CD concentrations of  $3.0 \times 10^{-3}$  and  $1.0 \times 10^{-2} \text{ mol dm}^{-3}$  is expected to be decreased to about 5 and 4% of the original concentration in the absence of DSP, respectively. This means that the icd signal intensity should be reduced to about 5 and 4% of the signal intensity in the absence of DSP, respectively, by the addition of DSP, if the ternary inclusion complex is not formed. This is not true. Consequently, the icd spectral changes by the addition of DSP (Figure 7) implies that the  $\gamma$ -CD-TMPyP-DSP inclusion complex is formed in solution containing  $\gamma$ -CD, TMPyP, and DSP. In the  $\gamma$ -CD-TMPyP-DSP system, there is an additional equilibrium besides the equilibria represented by Equations 1, 3, and 9.



where  $K_4$  is the equilibrium constant for the formation of the 1:1:1  $\gamma$ -CD-TMPyP-DSP inclusion complex ( $\gamma\text{-CD} \cdot \text{TMPyP} \cdot \text{DSP}$ ). The fluorescence intensity of TMPyP in solution containing  $\gamma$ -CD and DSP is represented as

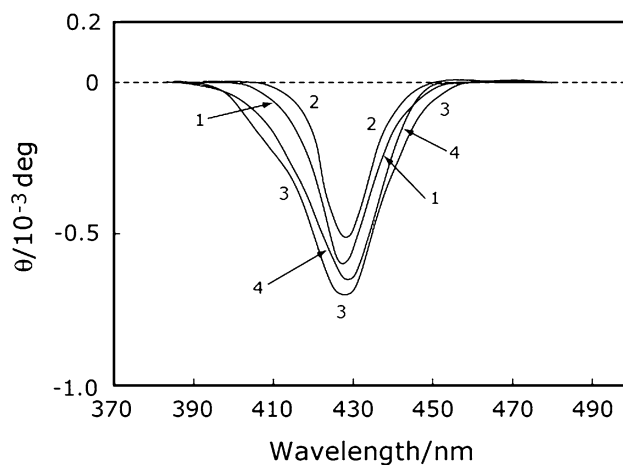


Figure 7. icd spectra of TMPyP ( $6.0 \times 10^{-6} \text{ mol dm}^{-3}$ ) in pH 7.3 buffers containing  $\gamma$ -CD and DSP. Concentrations of  $\gamma$ -CD and DSP: (1)  $[\gamma\text{-CD}] = 3.0 \times 10^{-3}$  and  $[\text{DSP}] = 0$ , (2)  $[\gamma\text{-CD}] = 3.0 \times 10^{-3}$  and  $[\text{DSP}] = 0.1$ , (3)  $[\gamma\text{-CD}] = 1.0 \times 10^{-2}$  and  $[\text{DSP}] = 0$ , and (4)  $[\gamma\text{-CD}] = 1.0 \times 10^{-2}$  and  $[\text{DSP}] = 0.1 \text{ mol dm}^{-3}$ .

$$\begin{aligned} I_f = & j[\text{TMPyP}] + k[\gamma\text{-CD} \cdot \text{TMPyP}] + l[(\text{TMPyP})_2] \\ & + m[\text{TMPyP} \cdot \text{DSP}] + n[\gamma\text{-CD} \cdot \text{TMPyP} \cdot \text{DSP}] \\ = & (j + kK_1[\gamma\text{-CD}] + lK_2[\text{TMPyP}] + mK_3[\text{DSP}] \\ & + nK_1K_4[\gamma\text{-CD}][\text{DSP}][\text{TMPyP}]) \end{aligned} \quad (13)$$

Here,  $j$ ,  $k$  ( $= 31.88j$ ),  $l$  ( $= 1080j$ ),  $m$  ( $= 15.48j$ ), and  $n$  are the constants including the fluorescence quantum yields of the TMPyP monomer, the 1:1  $\gamma$ -CD-TMPyP inclusion complex, the TMPyP dimer, the 1:1 TMPyP-DSP complex, and the 1:1:1  $\gamma$ -CD-TMPyP-DSP inclusion complex, respectively. The ratios  $k/j$  and  $m/j$  have been estimated from the simulations for the  $\gamma$ -CD-TMPyP system and the TMPyP-DSP system, respectively. Taking into account the mass balance of TMPyP, the following equation holds:

$$\begin{aligned} 2K_2[\text{TMPyP}]^2 + (1 + K_1[\gamma\text{-CD}] + K_3[\text{DSP}] \\ + K_1K_4[\gamma\text{-CD}][\text{DSP}][\text{TMPyP}] - [\text{TMPyP}]_0 = 0 \end{aligned} \quad (14)$$

Assuming a  $K_4$  value, the TMPyP monomer concentration can be calculated from Equation 14, because the  $K_1$ ,  $K_2$ , and  $K_3$  values have already been estimated. The fluorescence intensity is evaluated from Equation 13, under the assumption of the variables,  $j$ ,  $n$ , and  $K_4$ . A simulation has been performed for the fluorescence intensities obtained for the TMPyP ( $2.0 \times 10^{-6} \text{ mol dm}^{-3}$ ) solutions containing DSP ( $1.0 \times 10^{-2} \text{ mol dm}^{-3}$ ) and  $\gamma$ -CD (Figure 8). In Figure 8, the best fit simulation curve (curve 1), for which the values of  $j$ ,  $n$ , and  $K_4$  are assumed to be  $2.50 \times 10^6$ ,  $7.02 \times 10^7$ , and  $223 \text{ mol}^{-1} \text{ dm}^3$ , respectively, well fits the observed data.

Furthermore, we have evaluated a  $K_4$  value using the same simulation method, except for a DSP concentration of  $3.0 \times 10^{-2} \text{ mol dm}^{-3}$ . In this case, a  $K_4$  value has been evaluated to be  $172 \text{ mol}^{-1} \text{ dm}^3$ , which is similar to the  $K_4$  value ( $223 \text{ mol}^{-1} \text{ dm}^3$ ) estimated at a DSP concentration of  $1.0 \times 10^{-2} \text{ mol dm}^{-3}$ . In addition, we have further simulated the fluorescence intensity on the basis

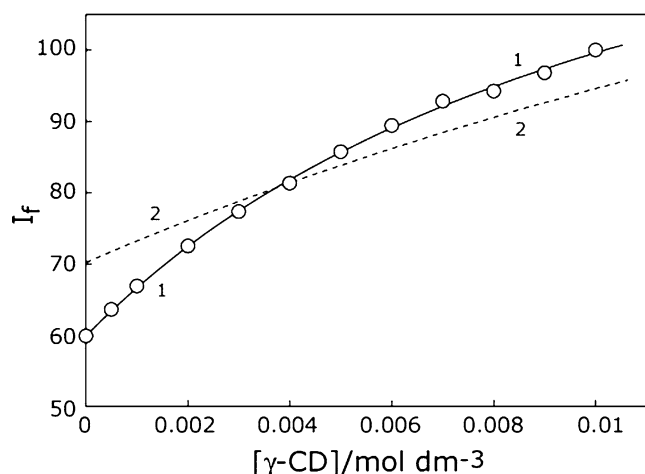


Figure 8. Simulation for the observed fluorescence intensities of TMPyP solution containing DSP. The best fit simulation curve (curve 1) has been based on the scheme involving the formation of the  $\gamma$ -CD–TMPyP–DSP inclusion complex. The best fit simulation curve (curve 2), which has been based on the scheme not involving the formation of the  $\gamma$ -CD–TMPyP–DSP inclusion complex, has been calculated with a proportionality constant of  $2.93 \times 10^7 \text{ mol}^{-1} \text{ dm}^3$ .  $[\text{TMPyP}]_0 = 2.0 \times 10^{-6} \text{ mol dm}^{-3}$ .  $[\text{DSP}] = 1.0 \times 10^{-2} \text{ mol dm}^{-3}$ .  $\lambda_{\text{ex}} = 426 \text{ nm}$ .  $\lambda_{\text{obs}} = 660 \text{ nm}$ .

of another scheme, in which the ternary  $\gamma$ -CD–TMPyP–DSP inclusion complex is not involved; the  $\gamma$ -CD–TMPyP inclusion complex and the 1:1 TMPyP–DSP complexes are alone formed. Figure 8 also exhibits the best fit simulation curve (curve 2) derived from the latter scheme, which does not reproduce the observed data. This confirms the formation of the  $\gamma$ -CD–TMPyP–DSP inclusion complex.

The  $K_4$  and  $K_3$  values are the equilibrium constants for the formation of the TMPyP–DSP complex with and without  $\gamma$ -CD, respectively. Nonetheless, the  $K_3$  and  $K_4$  values are close to each other. The analogous values for  $K_3$  and  $K_4$  may imply that a DSP molecule associates with TMPyP in nearly the same position on a TMPyP molecule, irrespective of whether TMPyP is bound or not bound to the  $\gamma$ -CD cavity. Consequently, it is most likely that the DSP molecule in the ternary  $\gamma$ -CD–TMPyP–DSP inclusion complex is not incorporated into the  $\gamma$ -CD cavity. When  $\gamma$ -CD shallowly accommodates an *N*-methylpyridyl moiety of TMPyP, it is unlikely that  $\gamma$ -CD prevents the association of DSP with TMPyP. The peak wavelength in the icd spectra of TMPyP in the presence of  $\gamma$ -CD and DSP is nearly the same as that in the presence of only  $\gamma$ -CD. This finding may support that the  $\gamma$ -CD cavity does not simultaneously accommodate TMPyP and DSP in the  $\gamma$ -CD–TMPyP–DSP inclusion complex.

For TMPyP in  $\alpha$ - or  $\beta$ -CD solution, absorption and fluorescence spectral changes similar to those for TMPyP in  $\gamma$ -CD solution were observed upon the addition of DSP. This finding suggests the formation of the ternary inclusion complex among CD, TMPyP, and DSP. From the simulations for the fluorescence intensity,  $K_4$  values of 175 and  $108 \text{ mol}^{-1} \text{ dm}^3$  have been evaluated for  $\alpha$ - and  $\beta$ -CD, respectively. Although the

$\gamma$ - and  $\gamma$ -CD cavities are narrower than the  $\gamma$ -CD cavity, the  $K_4$  values of the same order of magnitude as that for  $\gamma$ -CD have been estimated for  $\gamma$ - and  $\beta$ -CD. This supports that, in the CD–TMPyP–DSP inclusion complex, a DSP molecule associates with TMPyP outside the CD cavity.

## Conclusions

Although the interactions between  $\gamma$ -CD and a cationic porphyrin, TMPyP, are very weak compared to anionic porphyrins such as tetrakis(4-sulfonatophenyl)porphyrin,  $\gamma$ -CD forms the 1:1 inclusion complex with the TMPyP monomer in pH 7.3 buffer. The TMPyP monomer also forms the 1:1 organic cation–organic anion complexes with DSP. In addition, the 1:1  $\gamma$ -CD–TMPyP complex forms the ternary inclusion complex with DSP. In the ternary  $\gamma$ -CD–TMPyP–DSP inclusion complex, a DSP molecule is not incorporated into the  $\gamma$ -CD cavity. As in the case of  $\gamma$ -CD,  $\alpha$ - and  $\beta$ -CD form the 1:1 inclusion complex with the TMPyP monomer, and form the ternary inclusion complex with the TMPyP monomer and DSP.

## References

1. S. Mosseri, J.C. Mialocq, B. Perly, and P. Hambricht: *J. Phys. Chem.* **95**, 2196 (1991).
2. J.M. Ribo, J. Farrera, M.L. Valero, and A. Virgili: *Tetrahedron* **51**, 3705 (1995).
3. F. Venema, H.F.M. Nelissen, P. Berthault, N. Birlirakis, A.E. Rowan, M.C. Feiters, and R.J.M. Nolte: *Chem. Eur. J.* **4**, 2237 (1998).
4. S. Hamai and T. Koshiyama: *J. Photochem. Photobiol. A: Chem.* **127**, 135 (1999).
5. J. Mosinger, M. Deumie, K. Lang, P. Kubat, and D.M. Wagnerova: *J. Photochem. Photobiol. A: Chem.* **130**, 13 (2000).
6. S. Hamai and T. Koshiyama: *Spectrochim. Acta*, **57A**, 985 (2001).
7. Z. El-Hachemi, J. Farrera, H. Garcia-Ortega, O. Ramirez-Gutierrez, and J.M. Ribo: *J. Porphyrins Phthalocyanines* **5**, 465 (2001).
8. K. Kano, R. Nishiyabu, T. Asada, and Y. Kuroda: *J. Am. Chem. Soc.* **124**, 9937 (2002).
9. X. Wang, J. Pan, S. Shuang, and Y. Zhang: *Supramol. Chem.* **14**, 419 (2002).
10. K. Kano, N. Tanaka, H. Minamizono, and Y. Kawakita: *Chem. Lett.* 925 (1996).
11. K. Lang, P. Kubat, P. Lhotak, J. Mosinger, and D.M. Wagnerova: *Photochem. Photobiol.* **74**, 558 (2001).
12. G. Xiliang, S. Shaomin, D. Chuan, F. Feng, and M.S. Wong: *Spectrochim. Acta* **61A**, 413 (2005).
13. J.S. Manka and D.S. Lawrence: *J. Am. Chem. Soc.* **112**, 2440 (1990).
14. R.L. Schiller, J.H. Coates, and S.F. Lincoln: *J. Chem. Soc., Faraday Trans. 1* **80**, 1257 (1984).
15. S. Hamai: *Bull. Chem. Soc. Jpn.* **73**, 861 (2000).
16. S. Hamai and H. Satou: *Bull. Chem. Soc. Jpn.* **73**, 2207 (2000).
17. K. Kano, T. Nakajima, M. Takei, and S. Hashimoto: *Bull. Chem. Soc. Jpn.* **60**, 1281 (1987).
18. W.H. Tan, T. Ishikura, A. Maruta, T. Yamamoto, and Y. Matsui: *Bull. Chem. Soc. Jpn.* **71**, 2323 (1998).
19. S. Hamai: *Bull. Chem. Soc. Jpn.* **58**, 2099 (1985).
20. S. Hamai and H. Satou: *Bull. Chem. Soc. Jpn.* **75**, 77 (2002).
21. S. Hamai and K. Sato: *Dyes Pigm.* **57**, 15 (2003).
22. S. Hamai and H. Satou: *Spectrochim. Acta* **57**, 1745 (2001).
23. S. Hamai: *Bull. Chem. Soc. Jpn.* **75**, 2371 (2002).
24. S. Hamai: *Supramol. Chem.* **16**, 113 (2004).